THE JOURNAL OF PHYSICAL CHEMISTRY Letters

pubs.acs.org/JPCL

Letter

# Revealing High-Lying Intersystem Crossing in Brightly Luminescent Cyclic Trinuclear $Cu^I/Ag^I$ Complexes

Li-Rui Xing,[§] Zhou Lu,[§] Mian Li, Ji Zheng, and Dan Li*

Cite This: *J. Phys. Chem. Lett.* 2020, 11, 2067−2073

Read Online

ACCESS | Metrics & More | Article Recommendations | Supporting Information

**ABSTRACT:** The increased attention to luminescent copper(I) complexes, mostly mononuclear and dinuclear ones, in the past few years was mainly due to the new pathways established in the intersystem crossing (ISC) for highly efficient singlet/triplet harvesting, which showed great potential in light-emitting devices. Governing the photophysical processes of planar cyclic trinuclear complexes is more challenging owing to the rich intra- and intermolecular metal−metal interactions involved, but new opportunities also accompany this. Herein reported is a hidden route to the ultra-long-lived, highly efficient phosphorescence of cyclic trinuclear two-coordinate $Cu^I$−pyrazolate complexes through pushing the unfavorable metal-to-ligand charge transfer events to the high-lying ISC pathways. Moreover, an anomaly of much higher quantum yields of a trinuclear $Ag^I$−pyrazolate complex relative to its $Cu^I$ analogue is observed.

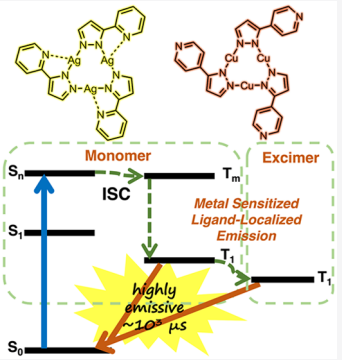




Researchers from both academic and industrial sectors have witnessed the remarkable advancements in luminescent $Cu^I$ complexes in the past decade owing to their prospect as low-cost, next-generation emitters for lighting and displays.[1,2] A ground-breaking mechanism promoted in this promising class of light-emitting materials was the feasibility of harvesting both singlet and triplet excitons through low-lying intersystem crossing (ISC) and subsequent reverse ISC (rISC), known as thermally activated delay fluorescence (TADF).[2−5]

Nevertheless, the rational design strategies[6−12] to acquire highly emissive $Cu^I$ complexes involving ISC/rISC processes appear to be in a dilemma. To ensure efficient ISC with a considerable radiative decay rate ($k_r$) requires the substantial involvement of copper in related singlet/triplet states to promote spin−orbit coupling (SOC).[6−8] On the contrary, the typical metal-to-ligand charge transfer (MLCT) events of $d^{10}$ metal centers, especially for low-coordinate ones, are associated with a large reorganization energy attributed to excited-state Jahn−Teller distortion; such an adverse effect should be minimized to bring down the nonradiative decay rate ($k_{nr}$).[9,10] Most recently, Thompson and coworkers successfully solved this conundrum in a family of mononuclear linear-coordinate $Cu^I$ complexes,[11,12] whose emissive lowest triplet states ($T_1$) are interligand excited states stabilized by the coplanar donor−acceptor ligands. A balance is achieved so that the metal contribution is large enough for effective ISC yet small enough to nearly eliminate nonradiative decay.[11]

As known, the SOC parameter of copper is about four times smaller than those of platinum and iridium.[13] A useful approach to counteract this inferior situation in promoting ISC is through polynuclear assemblies.[14−17] For example, Steffen, Cisnetti, and coworkers[14,15] as well as Costuas, Yam, Lescop, and coworkers[16] recently developed highly emissive dinuclear $Cu^I$ complexes, respectively, and demonstrated their rich supramolecular assemblies through Cu−Cu interactions.[17] These findings revealed that cuprophilic interactions can serve as a design motif for boosting the photoluminescence quantum yields ($\Phi_{PL}$) of $Cu^I$-based TADF or $T_1$ emitters through low-lying ISC paths with small single−triplet energy separation ($\Delta E_{S-T}$).

Cyclic trinuclear two-coordinate $d^{10}$ metal (i.e., $Cu^I/Ag^I/Au^I$) complexes represent a well-known family owing to their planar structures giving rise to intermolecular metal−metal interactions that are responsible for the tunable excimer emissions.[18−25] To date, most of them are found to be $T_1$ emitters, which have low-lying triplet metal-to-metal charge transfer or metal-centered ($^3$MMCT/$^3$MC) states.[18−20,22,24,26] Herein we report the unusual efficient high-lying ISC processes identified in some trinuclear $Cu^I/Ag^I$−pyrazolates, denoted as **Cu-2**, **Ag-2**, and **Cu-4** (Scheme 1), in which the strong luminescence comes from ligand-centered ($^3$LC) $T_1$ states and the corresponding excimers. The design of pyridyl pyrazole ligands was inspired by the highly emissive ($\Phi_{PL}$ up to ∼81%) planar mononuclear $Pt^{II}$ complexes containing pyridyl/pyrizinyl pyrazole ligands,[27] which also form excimers

**Received:** November 16, 2019
**Accepted:** February 21, 2020
**Published:** February 21, 2020

**Scheme 1. Structures of Cyclic Trinuclear Complexes Present in This Work**

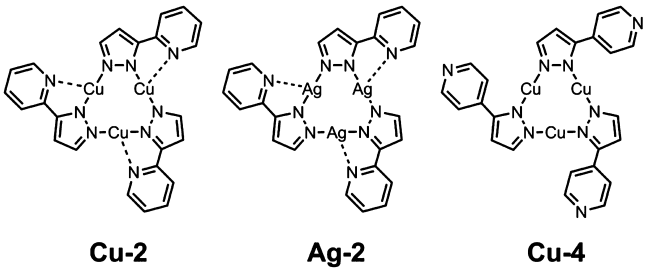


supported by intermolecular metal−metal interactions in the solid-state packing.

The solid samples of all target complexes were prepared in solvothermal reactions in good yields (see Experimental Procedures in the Supporting Information for details) and structurally characterized by X-ray crystallography (Tables S1−S3). The compositions of $M_3L_3$ (M = Cu/Ag, *H*L-2 = 3-(2′-pyridyl)-1*H*-pyrazole, *H*L-4 = 3-(4′-pyridyl)-1*H*-pyrazole) were confirmed.[28−30] The metal ions bridged by the pyrazolyl ligands share linear coordination geometry with different metal−metal distances and crystal packing modes (Figure 1, left; Figures S1−S6). For **Cu-2** and **Ag-2**, the chelating 2-pyridyl-N sites weakly coordinate to $Cu^I/Ag^I$ ions, enforcing the pyridyl and pyrazolyl rings to be almost coplanar, whereas **Cu-4** with 4-pyridyl, in the absence of weak coordination, deviates from the planar configuration. Notably, **Cu-2** shows a discrete dimer-of-trimer packing, with one set of intermolecular Cu−Cu distances (2.824 Å) approaching the sum of van der Waals radii (ca. 2.8 Å), whereas **Cu-4** stacks as a stair-like column. The coordination configuration and packing mode of **Ag-2** are similar to those of **Cu-2**, but the Ag−Ag contacts are weaker than the Cu analogues, which is common in the literature.[31−33]

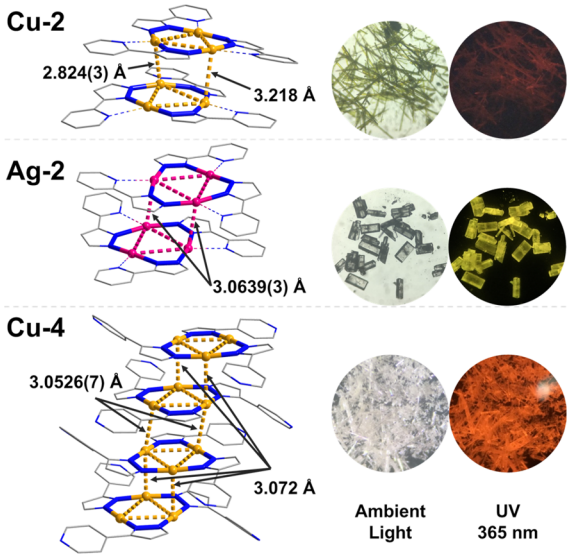


**Figure 1.** Left: Crystal structures of the three complexes at 100 K, marked with the shortest intermolecular metal−metal distances. Atom color codes: Cu, orange; Ag, magenta; C, gray; N, blue; H atoms are omitted. Right: Digital photographs of crystals under ambient light and hand-held 365 nm UV lamp, respectively, at room temperature.

Under ambient light, the crystalline sample of **Cu-2** shows a pale-yellow color, whereas those of **Ag-2** and **Cu-4** are colorless (Figure 1, right). When exposed to UV light, **Ag-2** and **Cu-4** glow brightly in yellow and orange, respectively, in stark contrast with **Cu-2**, which faintly displays orange light (Figure 1, right). The bulk samples of the complexes are poorly soluble in common solvents, and they are air-stable and thermally stable up to ca. 300 °C, indicated by thermogravimetric analysis (Figure S7). The bulk sample purity and phase homogeneity are ensured by elemental analysis and powder X-ray diffraction (Figures S8−S10).

The solid-state ultraviolet−visible absorption spectrum of **Cu-2** displays two peaks at 259 and 319 nm accompanied by a broad band located at 367 nm, whereas for **Ag-2** and **Cu-4** ,the absorption band peaks are 262, 316, and 316 (b, w) nm and 210, 293, and 293 (b) nm, respectively (Figure S30 and Table 1). Under low-energy excitation (400 nm for **Cu-2**, 370 nm for **Ag-2**, and 325 nm for **Cu-4**) at room temperature, the emission spectra of both **Cu-2** and **Cu-4** peak broadly and featurelessly around 650 nm (Figure 2a) with contrasting $\Phi_{PL}$ of 1.3 and 65%, respectively, whereas **Ag-2** displays a peak at 570 nm ($\Phi_{PL}$ = 25%). Compared with the triplet decays of **Cu-2** ($\tau_{av}$ = 5.8 $\mu$s, $k_r = 2.2 \times 10^3$ $s^{-1}$) and **Cu-4** ($\tau_{av}$ = 27.9 $\mu$s, $k_r = 2.3 \times 10^4$ $s^{-1}$), the decay lifetime of **Ag-2** is found to be ultralong ($\tau_{av}$ = 5833.7 $\mu$s, $k_r = 4.3 \times 10^1$ $s^{-1}$, Figure 2b).

Cooling to 77 K, the emission spectra behave drastically different. **Cu-2** shows a bathochromic shift of ca. 30 nm with the emission intensity vanishingly decreasing, which is attributed to the contraction of intertrimer Cu−Cu distances at low temperature (cf. Cu−Cu 2.900 Å at 293 K; 2.824 Å at 100 K), as commonly observed in the literature.[18−21] In contrast, **Ag-2** and **Cu-4** display high-energy, structured bands (~420−550 nm), indicative of vibrational transitions of the ligands, which coincide with their own infrared spectra (1464, 1498 $cm^{-1}$ for **Ag-2** and 1112, 1409 $cm^{-1}$ for **Cu-4**), and their low-energy bands remain almost intact at 77 K. For **Ag-2** and **Cu-4**, the new bands that appeared at 77 K also have ultralong decay lifetimes (e.g., $\tau_{av}$ = 1006.1 $\mu$s for the 470 nm band of **Ag-2**; $\tau_{av}$ = 770.2 $\mu$s for the 452 nm band of **Cu-4**), which are assigned as $^3$LC-based $T_1$ emissions. The structureless low-energy bands are attributed to corresponding excimers with drastically different lifetimes (e.g., $\tau_{av}$ = 5089.1 $\mu$s for the 570 nm band of **Ag-2**; $\tau_{av}$ = 27.68 $\mu$s for the 650 nm band of **Cu-4**, Table S7) due to the difference in the internal/external heavy-atom effect in Cu and Ag complexes.[35] The fact that the lifetimes of low-energy bands of **Ag-2** and **Cu-4** at room temperature are even slightly longer than those at 77 K suggests the existence of thermal equilibrium.

The detailed photophysical data are summarized in Table 1. The above unusual spectral profiles resemble the observations made by Thompson and coworkers,[11,34] which are anomalous compared with the reported cyclic trinuclear $Cu^I/Ag^I$−pyrazolates[18,19,24,25] in the following aspects.

(i) Metal effect: Usually $Cu^I$ complexes exhibit much brighter phosphorescence than $Ag^I$ analogues due to the internal heavy atom effect of Cu that facilitates fast ISC.[35] In fact, most trinuclear $Ag^I$−pyrazolates are barely emissive, but here **Ag-2** has much higher $\Phi_{PL}$ than **Cu-2.** Similarly, in the recent work by Thompson and coworkers[34] the $Ag^I$ complexes are as highly emissive as the $Cu^I$ complexes, but the decay lifetimes are in an unusual order Ag < Cu due to the smallest $\Delta E_{S-T}$ of the


https://dx.doi.org/10.1021/acs.jpclett.9b03382
J. Phys. Chem. Lett. 2020, 11, 2067−2073

**Table 1. Photophysical Data for the Three Complexes in the Solid State**

| complex | $T$/K | $\lambda_{abs}$/nm | $\lambda_{ex}$/nm | $\lambda_{em}$/nm[b] | $\tau/\mu s$[a] $\tau_1$ [$A_1$] | $\tau_2$ [$A_2$] | $\tau_{av}$ | $\Phi_{PL}$[c] | $k_r/s^{-1}$ | $k_{nr}/s^{-1}$ |
|---|---|---|---|---|---|---|---|---|---|---|
| **Cu-2** | 298 | 259, 319, 367 (b) | [d] | 655 | 2.0 [0.414] | 8.5 [0.586] | 5.8 | 0.013 | $2.2 \times 10^3$ | $1.7 \times 10^5$ |
| | 77 | | | 688 | 3.1 [0.341] | 9.2 [0.659] | 7.1 | [d] | | |
| **Ag-2** | 298 | 262, 316, 316 (b, w) | 363 | 570 | 200 [0.027] | 5990 [0.973] | 5833.7 | 0.25 | $4.3 \times 10^1$ | $1.3 \times 10^2$ |
| | 77 | | | (HE, structured) 438, 468, 503; (LE) 570 | 213.6[e] [0.627] | 2338.3[e] [0.373] | 1006.1 | 0.37 | $3.7 \times 10^2$ | $6.3 \times 10^2$ |
| **Cu-4** | 298 | 210, 293, 293 (b) | 325 | 650 | 27.9 [1] | | 27.9 | 0.65 | $2.3 \times 10^4$ | $1.3 \times 10^4$ |
| | 77 | | | (HE, structured) 425, 452, 476, 510; (LE) 654 | 203.1[f] [0.309] | 1023.8[f] [0.691] | 770.2 | 0.47 | $6.1 \times 10^2$ | $6.9 \times 10^2$ |

[a]$\tau$ = emission lifetime, $A$ = contribution factor, $\tau_{av} = \Sigma(A_i\tau_i)$. [b]Excitation wavelength: 400 nm for **Cu-2**, 370 nm for **Ag-2**, and 325 nm for **Cu-4**. [c]Absolute quantum yield. [d]Too weakly emissive to measure excitation and quantum yield. [e]Monitored emission peak: 468 nm. [f]Monitored emission peak: 452 nm. Abbreviations: HE = high-energy band, LE = low-energy band, b = broad, w = weak.

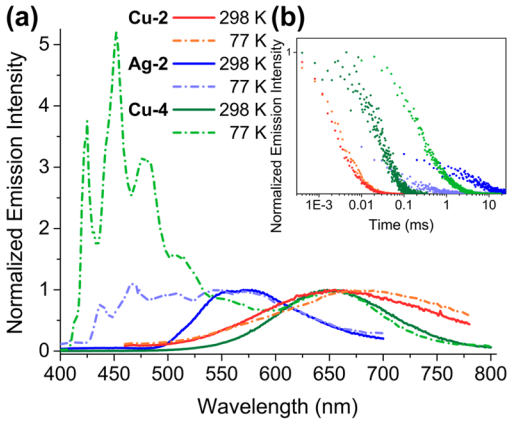


**Figure 2.** (a) Solid-state emission spectra at 298 and 77 K. (See Table 1 for excitation wavelengths.) The emission intensities are normalized with respect to the low-energy bands. (b) Corresponding decay lifetime semilog profiles of the three complexes at 298 and 77 K.

$Ag^I$ complexes, on the contrary to the situation in the present work.

(ii) Ligand effect: The initial design on the 2-pyridyl was to utilize its weak coordination with the metal ions to enforce the whole molecule in a coplanar conformation. It was expected that the $^3$LC states would stabilize through conjugation and also benefit the coupling of metal d orbitals and ligand $\pi$ orbitals to promote ISC efficiency.[11,12,36,37] However, the curved **Cu-4** with 4-pyridyl has a much higher $\Phi_{PL}$ than the flat **Cu-2**.

(iii) Supramolecular effect: Usually for cyclic trinuclear complexes, the emission profiles are governed by intermolecular metal−metal interactions.[18−25] In this work, the fact that **Cu-2** has the shortest Cu−Cu distances may be related to its lowest energy of the excimer band among the three complexes but cannot account for the absence of the high-energy ligand-localized band as well as its lowest $\Phi_{PL}$. We speculate that hidden ISC paths may be working.

Accordingly, time-dependent density functional theory (TD-DFT) calculations were performed to figure out the intricate ISC pathways (see the Computational Details in the Supporting Information), from which the low-energy excitation for the three complexes (see Table 1) is mainly assigned to MLCT origin. For **Cu-2**, a dimer-of-trimers model was used because only a low-energy, featureless band was recorded, which is attributed to the excimer emission supported by close Cu−Cu contacts.[27] Both the lowest excited single state ($S_1$) and $T_1$ are assigned to [Cu($d_z^2$) → $\pi^*$(py−pz)] (i.e., $^{1,3}$MLCT, Figure 3a; Tables S9 and S10), affirming our ligand design on the chelating 2-pyridyl groups,[27] but such MLCT events associated with low-lying ISC would cause unwanted nonradiative loss. In contrast, the dimer-of-trimers **Ag-2** and **Cu-4** have $^3$LC-based $T_1$ states (Table S16); for their monomer models, denoted as **Ag-2-*m*** and **Cu-4-*m***, the $^1$MLCT [Ag/Cu($d_z^2$) → $\pi^*$(py−pz)] $S_1$ and $^3$LC [$\pi$(py−pz) → $\pi^*$(py−pz)] $T_1$ states are assigned (Figure 3a; Tables S11−S14).

The experimental excitation energy of **Cu-2** (∼400 nm) is much lower than that of **Cu-4** (∼325 nm) as well as **Ag-2** (∼370 nm), which coincide with identified $^1$MLCT states of considerable oscillator strengths ($f$) in the calculations (Figure 3a). If **Ag-2** and **Cu-4** can undergo low-lying ISC paths following fast internal conversion after excitation, then the involved ISC must be very efficient, given that they exhibit very strong luminescence. However, such an efficient low-lying $^{1,3}$MLCT-based ISC route is lacking for **Ag-2** and **Cu-4**, which can also explain the anomaly of the much higher $\Phi_{PL}$ of **Ag-2** relative to **Cu-2** at room temperature. In the work by Thompson and coworkers,[11,34] the highly emissive $Ag^I$ complexes, undergoing low-lying ISC paths, have larger $k_r$ values than those of $Cu^I$ analogues. In contrast, here $\Phi_{PL}$ **Ag-2** ≫ **Cu-2** is not due to a larger $k_r$ but rather a $k_{nr}$ that is three orders of magnitude smaller (**Ag-2** $1.3 \times 10^2$ $s^{-1}$ vs **Cu-2** $1.7 \times 10^5$ $s^{-1}$). Taking all of this into account, the existence of low-lying ISC for **Ag-2** and **Cu-4** should be undermined.

In principle, the ISC rate is proportional to $|\langle S_n|H_{SOC}|T_m\rangle|^2/((\Delta E_{S-T})^2)$;[38] therefore, larger SOC matrix elements $\langle S_n|H_{SOC}|T_m\rangle$, smaller adiabatic $\Delta E_{S-T}$, and larger $f$ values can contribute to efficient ISC. Moreover, different d orbitals are required for spin-allowed ISC between coupled $^{1,3}$MLCT states.[39,40] Albeit very time-consuming, the SOC matrix elements covering the high-lying ISC pathways were calculated for the three complexes (Computational Details in the Supporting Information, Tables S24−S26). For **Cu-2**, the pathways involving low-lying $^{1,3}$MLCT states, predominantly the $S_1$ → $T_4/T_5$ transition with a relatively larger $f$ value, are reckoned as the major ISC processes. For **Ag-2-*m*** and **Cu-4-*m***, the $f$ values for the $S_1$ states ($^1$MLCT) are negligible. When looking into higher singlet states ($S_n$) with considerable $f$ values, multiple


https://dx.doi.org/10.1021/acs.jpclett.9b03382
J. Phys. Chem. Lett. 2020, 11, 2067−2073

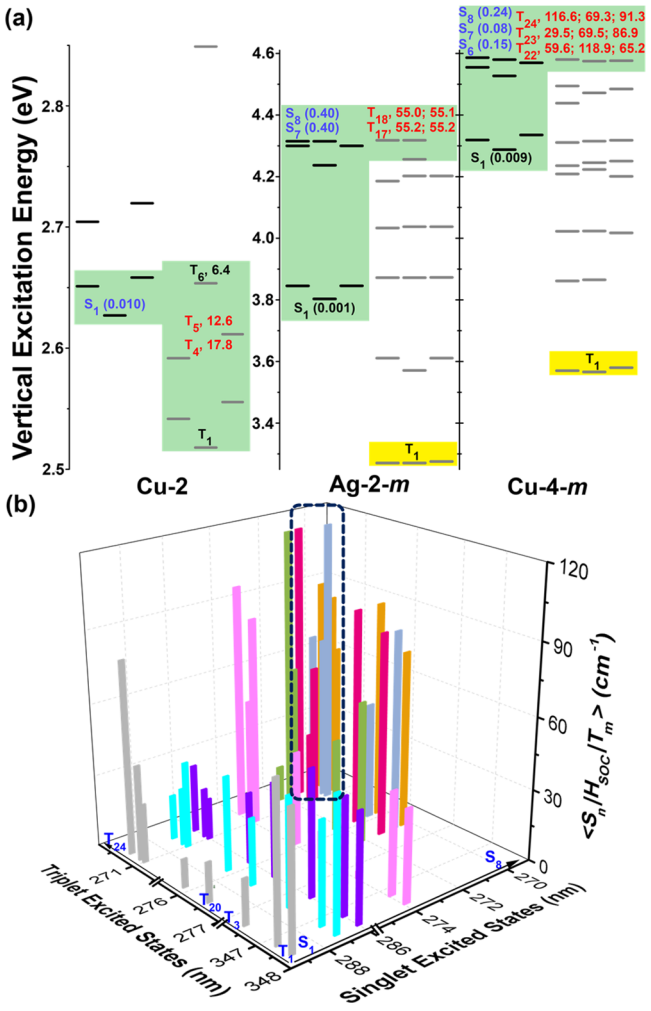


**Figure 3.** (a) Selected singlet ($S_n$, marked in blue) and triplet ($T_m$, marked in red) states experiencing ISC processes. The values in the parentheses represent the oscillator strengths of $S_n$, and the numbers following $T_m$ represent the values of SOC matrix elements (in $cm^{-1}$) of the efficient ISC channels. The MLCT- and LC-dominated excited states are highlighted in green and yellow regions, respectively. (b) Three-dimensional diagram of selected SOC matrix elements for **Cu-4-*m*** between $S_n$ ($n$ = 1−8) and $T_m$ ($m$ = 1−3, 20−24) states. Colors refer to different $S_n$ states involved in ISC channels. Proposed efficient high-lying ISC pathways are circled in a dashed line.

high-lying $^{1,3}$MLCT-based ISC channels for **Ag-2-*m***, viz. $S_7$, $S_8$ → $T_{17}$, $T_{18}$, and **Cu-4-*m***, viz. $S_6$, $S_7$, and $S_8$ → $T_{22}$, $T_{23}$, and $T_{24}$, are revealed.

In Figure 3a, the selected ISC pathways are marked with corresponding $f$ and SOC matrix element values. Although hidden in high-lying $S_n$ → $T_m$ paths, **Ag-2-*m*** and **Cu-4-*m*** have four or more significant SOC matrix element values compared with **Cu-2** having smaller SOC matrix element values in low-lying paths. The selected SOC matrix element values for **Cu-4-*m*** are depicted in Figure 3b, showing the most probable high-lying ISC pathways. Although the SOC parameter of Cu (857 $cm^{-1}$) is smaller than that of Ag (1779 $cm^{-1}$), the external heavy atom effect of silver causes it to contribute to the SOC to a lesser extent relative to copper.[35] As a result, **Cu-4** exhibits orders of magnitude larger values of both $k_r$ and $k_{nr}$ compared with those of **Ag-2** at room temperature (Table 1), giving the highest quantum yield of 65% for **Cu-4** at room temperature among the three complexes.

Another key factor governing ISC processes is the adiabatic $\Delta E_{S-T}$ value. A prerequisite for ISC/rISC to take place is a $\Delta E_{S-T}$ value not larger than 1000 $cm^{-1}$,[3,6,41] and when it is small enough to influence the rate of ISC, then the competition of high-lying ISC with internal conversion and low-lying ISC may occur, followed by $^3$LC-based $T_1$ emission, as previously pointed out by Thompson, Yersin, and coworkers.[42,43] In the work by Thompson and coworkers,[11,34] the $\Delta E_{S-T}$ values of $Ag^I$ complexes (150−180 $cm^{-1}$) are smaller than those of $Cu^I$ complexes (570−590 $cm^{-1}$). Here the $\Delta E_{S-T}$ values of **Ag-2-*m*** (~24.2 $cm^{-1}$) and **Cu-4-*m*** (0−95.6 $cm^{-1}$) through multiple paths in high-lying ISC are very small, even negligible, compared with those of **Cu-2** (124.9 and 283.4 $cm^{-1}$) through low-lying paths.

The final emissive states of **Ag-2** and **Cu-4** are $^3$LC-based $T_1$ states and corresponding excimers, experiencing thermal equilibrium, which is consistent with the ultralong lifetimes for **Ag-2** and **Cu-4**. Previously the origin of the excimer in such type of cyclic trinuclear complexes was found to be $^3$MC, and there were only broad bands (i.e., that of excimer) identified with varying emission wavelengths, which are temperature-sensitive due to the formation of excited-state metal−metal bonding.[20,21,44] In the present work, the origin of monomer emission (high-energy band) is found to be $^3$LC, and thus the excimer emission (low-energy band) can be simultaneously observed and is temperature-insensitive (see Figure 2a) due to the absence of intermolecular metal−metal bonding, which is supported by TD-DFT calculations of $T_1$ geometry (Tables S15 and S16). The situation here is more like the classic organic pyrene excimer for which dual emissions from both monomer and excimer can be observed under the same excitation wavelength.[45,46]

The internal reorganization energies were also calculated to evaluate the de-excitation processes ($T_1$ → $S_0$, Table S17), giving a larger energy loss of vibration relaxation for **Cu-2** (0.58 eV) than for **Ag-2** (0.43 eV) and **Cu-4** (0.52 eV). In combination with the contribution of high-lying ISC processes that reduces the adverse effect of the MLCT events, the nonradiative decay loss of **Ag-2** and **Cu-4** is then much lower than that of **Cu-2** (see Table 1).

The present study uncovers a hidden route of high-lying ISC to obtain ultralong-lived, highly emissive cyclic trinuclear $Cu^I$/$Ag^I$−pyrazolate complexes. The conventional cyclic trinuclear complexes, such as $[Cu(3,5\text{-}(CF_3)_2\text{−pyrazolate})]_3$, which exhibits high quantum efficiency,[18−20,22] form excited-state Cu−Cu bonding and undergo a $S_0$ ↔ $T_1$ spin-forbidden transition, giving $^3$MC $T_1$ states (Scheme 2a). Here the MLCT states, familiar for mononuclear square-planar $d^8$ ($Pt^{II}$, $Pd^{II}$, and $Au^{III}$) complexes, are introduced to trinuclear linear or T-shaped $d^{10}$ ($Cu^I$ and $Ag^I$) complexes, although it would cause unwanted nonradiative loss due to excited state Jahn−Teller distortion and vibronic coupling through low-lying ISC, resulting in low quantum efficiency, as in the case of **Cu-2** (Scheme 2b).

For **Ag-2** or **Cu-4** excited as a monomer, the unfavorable MLCT events are pushed to the high-lying ISC pathways, and the $^3$LC are stabilized as the $T_1$ states (Scheme 2c). Subsequently, the triplet excitons are efficiently harvested through dual emissions, that is, high-energy $^3$LC and low-energy excimer bands that are subject to thermal equilibrium. At low temperature, both a high-energy structured band and a low-energy broad band can be observed; upon heating, the excitons from the monomer can step over the energy barrier to


https://dx.doi.org/10.1021/acs.jpclett.9b03382
J. Phys. Chem. Lett. 2020, 11, 2067−2073

**Scheme 2. Proposed Jablonski Diagrams for Cyclic Trinuclear Complexes (a) [Cu(3,5-$(CF_3)_2$−Pyrazolate)]$_3$, (b) Cu-2, and (c) Ag-2 and Cu-4**[a]

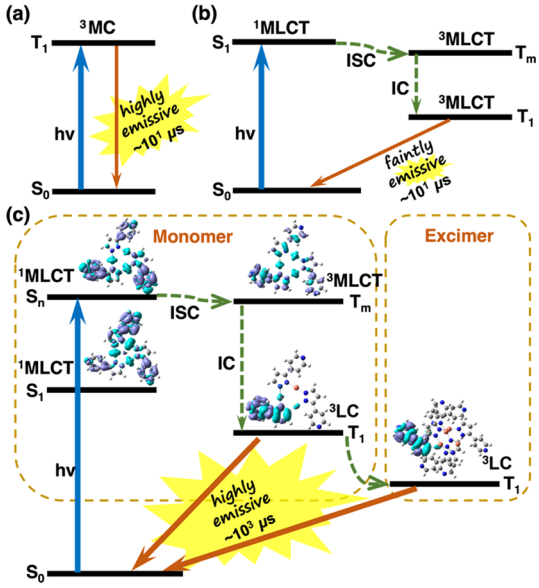


[a]ISC = intersystem crossing, IC = internal conversion. MC = metal-centered, MLCT = metal-to-ligand charge transfer, LC = ligand centered. Radiative transitions are shown by solid arrows, whereas nonradiative transitions are shown by dotted arrows. *n* and *m* are integer numbers (≥2).

effectively populate excimer states, and hence only the low-energy emission band is observed at room temperature. Note that for **Cu-4** the quantum yield is even higher at room temperature (cf. 65% at 298 K; 47% at 77 K).

The photophysical scenario outlined here, in which a substantial metal contribution is retained for effective ISC while the concomitant nonradiative decay is masked to some extent, provides an alternative solution to the dilemma in designing highly emissive $d^{10}$ metal complexes, among several other approaches, including triplet harvesting through a multinuclear strategy,[47] singlet harvesting through TADF,[48] a heterometallic strategy,[22] metal adducting,[49] and so on.[50]

## ■ ASSOCIATED CONTENT

### Supporting Information

The Supporting Information is available free of charge at https://pubs.acs.org/doi/10.1021/acs.jpclett.9b03382.

Details of experimental procedures, physical characterizations, crystallographic data, computational details and results, Figures S1−S39, and Tables S1−S35 (PDF)

Crystallography data for **Cu-2**, **Ag-2**, and **Cu-4** at 100 and 293 K (CIF)

## ■ AUTHOR INFORMATION


### Corresponding Author

**Dan Li** − *College of Chemistry and Materials Science, Jinan University, Guangzhou 510632, P. R. China;* orcid.org/0000-0002-4936-4599; Email: danli@jnu.edu.cn

### Authors

**Li-Rui Xing** − *Department of Chemistry, Shantou University, Shantou, Guangdong 515063, P. R. China*

**Zhou Lu** − *College of Chemistry and Materials Science, Jinan University, Guangzhou 510632, P. R. China;* orcid.org/0000-0002-6447-4905

**Mian Li** − *Department of Chemistry, Shantou University, Shantou, Guangdong 515063, P. R. China;* orcid.org/0000-0003-1293-3636

**Ji Zheng** − *College of Chemistry and Materials Science, Jinan University, Guangzhou 510632, P. R. China*

Complete contact information is available at: https://pubs.acs.org/10.1021/acs.jpclett.9b03382

### Author Contributions

[§]L.-R.X. and Z.L. contributed equally.


### Notes

The authors declare no competing financial interest.

## ■ ACKNOWLEDGMENTS

This work is financially supported by the National Natural Science Foundation of China (21731002 and 91222202) and the Major Program of Guangdong Basic and Applied Research (no. 2019B030302009). We thank Dr. Jun Liu for the discussion on theoretical calculations and Mr. Yonghong Xiao for the help with crystallography studies.

## ■ REFERENCES


(1) Yam, V. W.-W.; Au, V. K.-M.; Leung, S. Y.-L. Light-emitting self-assembled materials based on $d^8$ and $d^{10}$ transition metal complexes. *Chem. Rev.* **2015**, *115*, 7589−7728.

(2) Yersin, H.; Czerwieniec, R.; Shafikov, M. Z.; Suleymanova, A. F. *Highly Efficient OLEDs Materials Based on Thermally Activated Delayed Fluorescence*; Wiley-VCH Verlag GmbH & Co. KGaA, 2019; pp 1−60.

(3) Yersin, H.; Czerwieniec, R.; Shafikov, M. Z.; Suleymanova, A. F. TADF material design: photophysical background and case studies focusing on $Cu^I$ and $Ag^I$ complexes. *ChemPhysChem* **2017**, *18*, 3508−3535.

(4) Cariati, E.; Lucenti, E.; Botta, C.; Giovanella, U.; Marinotto, D.; Righetto, S. Cu(I) hybrid inorganic−organic materials with intriguing stimuli responsive and optoelectronic properties. *Coord. Chem. Rev.* **2016**, *306*, 566−614.

(5) Leitl, M. J.; Zink, D. M.; Schinabeck, A.; Baumann, T.; Volz, D.; Yersin, H. Copper(I) complexes for thermally activated delayed fluorescence: from photophysical to device properties. *Top. Curr. Chem.* **2016**, *374*, 25.

(6) Hofbeck, T.; Monkowius, U.; Yersin, H. Highly efficient luminescence of Cu(I) compounds: thermally activated delayed fluorescence combined with short-lived phosphorescence. *J. Am. Chem. Soc.* **2015**, *137*, 399−404.

(7) Föller, J.; Kleinschmidt, M.; Marian, C. M. Phosphorescence or thermally activated delayed fluorescence? intersystem crossing and radiative rate constants of a three-coordinate copper(I) complex determined by quantum-chemical methods. *Inorg. Chem.* **2016**, *55*, 7508−7516.

(8) Aguiló, E.; Moro, A. J.; Outis, M.; Pina, J.; Sarmento, D.; Seixas de Melo, J. S.; Rodríguez, L.; Lima, J. C. Deactivation routes in gold(I) polypyridyl complexes: internal conversion vs fast intersystem crossing. *Inorg. Chem.* **2018**, *57*, 13423−13430.

(9) Hamze, R.; Jazzar, R.; Soleilhavoup, M.; Djurovich, P. I.; Bertrand, G.; Thompson, M. E. Phosphorescent 2-, 3- and 4-coordinate cyclic(alkyl)(amino)carbene (CAAC) Cu(I) complexes. *Chem. Commun.* **2017**, *53*, 9008−9011.

(10) Gernert, M.; Müller, U.; Haehnel, M.; Pflaum, J.; Steffen, A. A cyclic alkyl(amino)carbene as two-atom-π-chromophore leading to the first phosphorescent linear Cu(I) complexes. *Chem. - Eur. J.* **2017**, *23*, 2206−2216.

(11) Hamze, R.; Peltier, J. L.; Sylvinson, D.; Jung, M.; Cardenas, J.; Haiges, R.; Soleilhavoup, M.; Jazzar, R.; Djurovich, P. I.; Bertrand, G.;

Thompson, M. E. Eliminating nonradiative decay in Cu(I) emitters: > 99% quantum efficiency and microsecond lifetime. *Science* **2019**, *363*, 601−606.
(12) Shi, S.; Jung, M. C.; Coburn, C.; Tadle, A.; Sylvinson M. R., D.; Djurovich, P. I.; Forrest, S. R.; Thompson, M. E. Highly efficient photo- and electroluminescence from two-coordinate Cu(I) complexes featuring nonconventional N-heterocyclic carbenes. *J. Am. Chem. Soc.* **2019**, *141*, 3576−3588.
(13) Fraga, S.; Karwowski, J.; Saxena, K. M. S. *Handbook of Atomic Data*; Elsevier, 1976.
(14) Nitsch, J.; Lacemon, F.; Lorbach, A.; Eichhorn, A.; Cisnetti, F.; Steffen, A. Cuprophilic interactions in highly luminescent dicopper(I)-NHC-picolyl complexes - fast phosphorescence or TADF? *Chem. Commun.* **2016**, *52*, 2932−2935.
(15) Hupp, B.; Nitsch, J.; Schmitt, T.; Bertermann, R.; Edkins, K.; Hirsch, F.; Fischer, I.; Auth, M.; Sperlich, A.; Steffen, A. Stimulus-triggered formation of an anion-cation exciplex in copper(I) complexes as a mechanism for mechanochromic phosphorescence. *Angew. Chem., Int. Ed.* **2018**, *57*, 13671−13675.
(16) El Sayed Moussa, M.; Evariste, S.; Wong, H.-L.; Le Bras, L.; Roiland, C.; Le Polles, L.; Le Guennic, B.; Costuas, K.; Yam, V. W.-W.; Lescop, C. A solid state highly emissive Cu(I) metallacycle: promotion of cuprophilic interactions at the excited states. *Chem. Commun.* **2016**, *52*, 11370−11373.
(17) Evariste, S.; Khalil, A. M.; Moussa, M. E.; Chan, A. K.-W.; Hong, E. Y.-H.; Wong, H.-L.; Le Guennic, B.; Calvez, G.; Costuas, K.; Yam, V. W.-W.; Lescop, C. Adaptive coordination-driven supramolecular syntheses toward new polymetallic Cu(I) luminescent assemblies. *J. Am. Chem. Soc.* **2018**, *140*, 12521−12526.
(18) Dias, H. V. R.; Diyabalanage, H. V. K.; Eldabaja, M. G.; Elbjeirami, O.; Rawashdeh-Omary, M. A.; Omary, M. A. Brightly phosphorescent trinuclear copper(I) complexes of pyrazolates: substituent effects on the supramolecular structure and photophysics. *J. Am. Chem. Soc.* **2005**, *127*, 7489−7501.
(19) Omary, M. A.; Rawashdeh-Omary, M. A.; Gonser, M. W. A.; Elbjeirami, O.; Grimes, T.; Cundari, T. R.; Diyabalanage, H. V. K.; Gamage, C. S. P.; Dias, H. V. R. Metal effect on the supramolecular structure, photophysics, and acid−base character of trinuclear pyrazolato coinage metal complexes. *Inorg. Chem.* **2005**, *44*, 8200−8210.
(20) Vorontsov, I. I.; Kovalevsky, A. Y.; Chen, Y.-S.; Graber, T.; Gembicky, M.; Novozhilova, I. V.; Omary, M. A.; Coppens, P. Shedding light on the structure of a photoinduced transient excimer by time-resolved diffraction. *Phys. Rev. Lett.* **2005**, *94*, 193003.
(21) Grimes, T.; Omary, M. A.; Dias, H. V. R.; Cundari, T. R. Intertrimer and intratrimer metallophilic and excimeric bonding in the ground and phosphorescent states of trinuclear coinage metal pyrazolates: a computational study. *J. Phys. Chem. A* **2006**, *110*, 5823−5830.
(22) Galassi, R.; Ghimire, M. M.; Otten, B. M.; Ricci, S.; McDougald, R. N., Jr.; Almotawa, R. M.; Alhmoud, D.; Ivy, J. F.; Rawashdeh, A.-M. M.; Nesterov, V. N.; Reinheimer, E. W.; Daniels, L. M.; Burini, A.; Omary, M. A. Cupriphication of gold to sensitize $d^{10}$−$d^{10}$ metal−metal bonds and near-unity phosphorescence quantum yields. *Proc. Natl. Acad. Sci. U. S. A.* **2017**, *114*, E5042−E5051.
(23) Ni, W.-X.; Li, M.; Zheng, J.; Zhan, S.-Z.; Qiu, Y.-M.; Ng, S. W.; Li, D. Approaching white-light emission from a phosphorescent trinuclear gold(I) cluster by modulating its aggregation behavior. *Angew. Chem., Int. Ed.* **2013**, *52*, 13472−13476.
(24) Xiao, Q.; Zheng, J.; Li, M.; Zhan, S.-Z.; Wang, J.-H.; Li, D. Mechanically triggered fluorescence/phosphorescence switching in the excimers of planar trinuclear copper(I) pyrazolate complexes. *Inorg. Chem.* **2014**, *53*, 11604−11615.
(25) Yang, H.; Zheng, J.; Peng, S.-K.; Zhu, X.-W.; Wan, M.-Y.; Lu, W.; Li, D. A chemopalette strategy for white light by modulating monomeric and excimeric phosphorescence of a simple Cu(I) cyclic trinuclear unit. *Chem. Commun.* **2019**, *55*, 4635−4638.
(26) Liu, Q.; Xie, M.; Chang, X.-Y.; Cao, S.; Zou, C.; Fu, W.-F.; Che, C.-M.; Chen, Y.; Lu, W. Tunable multicolor phosphorescence of crystalline polymeric complex salts with metallophilic backbones. *Angew. Chem., Int. Ed.* **2018**, *57*, 6279−6283.
(27) Ly, K. T.; Chen-Cheng, R.-W.; Lin, H.-W.; Shiau, Y.-J.; Liu, S.-H.; Chou, P.-T.; Tsao, C.-S.; Huang, Y.-C.; Chi, Y. Near-infrared organic light-emitting diodes with very high external quantum efficiency and radiance. *Nat. Photonics* **2017**, *11*, 63−68.
(28) Singh, K.; Long, J. R.; Stavropoulos, P. Ligand-unsupported metal−metal (M = Cu, Ag) interactions between closed-shell $d^{10}$ trinuclear systems. *J. Am. Chem. Soc.* **1997**, *119*, 2942−2943.
(29) Li, R. Bis{tris[$\mu$-2-(1*H*-pyrazol-3-yl-$\kappa N1$:$\kappa N^2$)pyridinato-$\kappa N$]-trisilver(I)}(2 *Ag*—*Ag*). *Acta Crystallogr., Sect. E: Struct. Rep. Online* **2007**, *63*, m1640.
(30) An, Z.; Zhou, R.-J. *Cyclo*-tris[$\mu$-5-(2-pyridyl)pyrazol-1-ido-$\kappa^3N^1$,$N^5$:$N^2$]trisilver(I). *Acta Crystallogr., Sect. E: Struct. Rep. Online* **2009**, *65*, m1335.
(31) Rasika Dias, H. V.; Polach, S. A.; Wang, Z. Coinage metal complexes of 3,5-bis(trifluoromethyl)pyrazolate ligand. *J. Fluorine Chem.* **2000**, *103*, 163−169.
(32) Rasika Dias, H. V.; Palehepitiya Gamage, C. S. Arene-sandwiched silver(I) pyrazolates. *Angew. Chem., Int. Ed.* **2007**, *46*, 2192−2194.
(33) Dias, H. V. R.; Gamage, C. S. P.; Keltner, J.; Diyabalanage, H. V. K.; Omari, I.; Eyobo, Y.; Dias, N. R.; Roehr, N.; McKinney, L.; Poth, T. Trinuclear silver(I) complexes of fluorinated pyrazolates. *Inorg. Chem.* **2007**, *46*, 2979−2987.
(34) Hamze, R.; Shi, S.; Kapper, S. C.; Muthiah Ravinson, D. S.; Estergreen, L.; Jung, M. C.; Tadle, A.; Haiges, R.; Djurovich, P. I.; Peltier, J. L.; Jazzar, R.; Bertrand, G.; Bradforth, S. E.; Thompson, M. E. "Quick-silver" from a systematic study of highly luminescent, two-coordinate, $d^{10}$ coinage metal complexes. *J. Am. Chem. Soc.* **2019**, *141*, 8616−8626.
(35) Hsu, C.-W.; Lin, C.-C.; Chung, M.-W.; Chi, Y.; Lee, G.-H.; Chou, P.-T.; Chang, C.-H.; Chen, P.-Y. Systematic investigation of the metal-structure−photophysics relationship of emissive $d^{10}$-complexes of group 11 elements: the prospect of application in organic light emitting devices. *J. Am. Chem. Soc.* **2011**, *133*, 12085−12099.
(36) Earl, L. D.; Nagle, J. K.; Wolf, M. O. Tuning the extended structure and electronic properties of gold(I) thienyl pyrazolates. *Inorg. Chem.* **2014**, *53*, 7106−7117.
(37) Di, D.; Romanov, A. S.; Yang, L.; Richter, J. M.; Rivett, J. P. H.; Jones, S.; Thomas, T. H.; Abdi Jalebi, M.; Friend, R. H.; Linnolahti, M.; Bochmann, M.; Credgington, D. High-performance light-emitting diodes based on carbene-metal-amides. *Science* **2017**, *356*, 159−163.
(38) Marian, C. M. Spin-orbit coupling and intersystem crossing in molecules. *Wiley Interdiscip. Rev.: Comput. Mol. Sci.* **2012**, *2*, 187−203.
(39) Li, E. Y.-T.; Jiang, T.-Y.; Chi, Y.; Chou, P.-T. Semi-quantitative assessment of the intersystem crossing rate: an extension of the El-Sayed rule to the emissive transition metal complexes. *Phys. Chem. Chem. Phys.* **2014**, *16*, 26184−26192.
(40) Penfold, T. J.; Gindensperger, E.; Daniel, C.; Marian, C. M. Spin-vibronic mechanism for intersystem crossing. *Chem. Rev.* **2018**, *118*, 6975−7025.
(41) Czerwieniec, R.; Leitl, M. J.; Homeier, H. H. H.; Yersin, H. Cu(I) complexes - thermally activated delayed fluorescence. photophysical approach and material design. *Coord. Chem. Rev.* **2016**, *325*, 2−28.
(42) Leitl, M. J.; Krylova, V. A.; Djurovich, P. I.; Thompson, M. E.; Yersin, H. Phosphorescence versus thermally activated delayed fluorescence. controlling singlet−triplet splitting in brightly emitting and sublimable Cu(I) compounds. *J. Am. Chem. Soc.* **2014**, *136*, 16032−16038.
(43) Schinabeck, A.; Leitl, M. J.; Yersin, H. Dinuclear Cu(I) complex with combined bright TADF and phosphorescence. zero-field splitting and spin−lattice relaxation effects of the triplet state. *J. Phys. Chem. Lett.* **2018**, *9*, 2848−2856.
(44) Hu, B.; Gahungu, G.; Zhang, J. Optical properties of the phosphorescent trinuclear copper(I) complexes of pyrazolates: insights from theory. *J. Phys. Chem. A* **2007**, *111*, 4965−4973.


https://dx.doi.org/10.1021/acs.jpclett.9b03382
*J. Phys. Chem. Lett.* 2020, 11, 2067−2073

(45) Turro, N. J. *Modern Molecular Photochemistry*; University Science Books, 1991.
(46) Hoche, J.; Schmitt, H.-C.; Humeniuk, A.; Fischer, I.; Mitrić, R.; Röhr, M. I. S. The mechanism of excimer formation: an experimental and theoretical study on the pyrene dimer. *Phys. Chem. Chem. Phys.* **2017**, *19*, 25002−25015.
(47) Dias, H. V. R.; Diyabalanage, H. V. K.; Ghimire, M. M.; Hudson, J. M.; Parasar, D.; Palehepitiya Gamage, C. S.; Li, S.; Omary, M. A. Brightly phosphorescent tetranuclear copper(i) pyrazolates. *Dalton Trans* **2019**, *48*, 14979−14983.
(48) Titov, A. A.; Filippov, O. A.; Smol'yakov, A. F.; Godovikov, I. A.; Shakirova, J. R.; Tunik, S. P.; Podkorytov, I. S.; Shubina, E. S. Luminescent complexes of the trinuclear silver(I) and copper(I) pyrazolates supported with bis(diphenylphosphino)methane. *Inorg. Chem.* **2019**, *58*, 8645−8656.
(49) Ni, W.-X.; Qiu, Y.-M.; Li, M.; Zheng, J.; Sun, R. W.-Y.; Zhan, S.-Z.; Ng, S. W.; Li, D. Metallophilicity-driven dynamic aggregation of a phosphorescent gold(I)−silver(I) cluster prepared by solution-based and mechanochemical approaches. *J. Am. Chem. Soc.* **2014**, *136*, 9532−9535.
(50) Zheng, J.; Yang, H.; Xie, M.; Li, D. The $\pi$-acidity/basicity of cyclic trinuclear units (CTUs): from a theoretical perspective to potential applications. *Chem. Commun.* **2019**, *55*, 7134−7146.



https://dx.doi.org/10.1021/acs.jpclett.9b03382
*J. Phys. Chem. Lett.* 2020, 11, 2067−2073